

2

STUDY OF ANGULAR AND SPECTRAL DISTRIBUTION OF
EARTH'S RADIATION IN THE INFRARED FIELD OF
SPECTRUM CONDUCTED FROM THE EARTH'S
EXPLORER "KOSMOS-45"

P.A. Bazhulin, A.V. Karmashev and M.N. Markov

(NASA-TT-F-14442) STUDY OF ANGULAR AND SPECTRAL DISTRIBUTION OF EARTH'S RADIATION IN THE INFRARED FIELD OF SPECTRUM CONDUCTED FROM THE EARTH'S EXPLORER P.A. Bazhulin, et al (NASA) Jun. 1972 38 p N72-32787 Unclas CSCL 03B G3/29 43817

Translation of "Issledovaniye uglovogo i spektralnogo raspredeleniya izlucheniya zemli v infrakrasnoy oblasti spektra s iz "kosmos-45", Kosmicheskiye issledovaniya (Cosmic Research), Vol. 4, No. 4, July and August 1966, pp. 601-618.



COSMIC RESEARCH

STUDY OF ANGULAR AND SPECTRAL DISTRIBUTION OF EARTH'S
RADIATION IN THE INFRARED FIELD OF SPECTRUM CONDUCTED FROM
THE EARTH'S EXPLORER "KOSMOS-45"

KOSMICHESKIE ISSLEDOVANIIA. VOL. 4 No. 4, 601-618

(July-Aug. 1966)

BY

BAZHULIN, P.A., KARMASHEV, A.V., and MARKOV, M.N.

The method and results of studies of Earth's radiation obtained during the flight of the Earth's Explorer "Kosmos-45" are described here. Data on angular (solution $2 \cdot 10^{-3}$ rad), spectral (in sections 0.8-4.5 micrometers, 4.5-38 micrometers, 4.5-8.5 micrometers, 8.5-12.5 micrometers) and geographic distributions of thermal radiation flows and albedo of the Earth are cited here. Information is supplied about surveyed flows of the infrared radiation of the ionosphere in the 0.8-4.5 and 4.5-8.5 micrometers field on the daytime side as well as on the nighttime side of the Earth. The presence of water vapor at the altitudes about 100 km has been established in areas of large aqueous surfaces on the Earth.

1. The method of investigating the Earth's atmosphere according to infrared radiation spectra surveyed from cosmic apparatus has been more often used in recent years. This method has significant features. First, there exists here a broad set of conditions in the atmosphere as far as the altitude (during rocket experiments), as well as the locality are concerned (during experiments with satellites). Second, owing to the rapid motion of cosmic apparatus, aboard which research apparatus are installed, these conditions undergo continuous and rapid changes. If the first circumstance happens to be very favorable, as it permits one to obtain statistical characteristics of the atmosphere during one experiment, so the second one superimposes very tough requirements on the rapid action of the equipment and the spatial results attained. Failure to fulfill these requirements may bring to nothing results of the experiment. It is important to have a good angular solution, as the apparatus and the object to be investigated, as a rule, are separated by considerable distances. For example, the angular dimensions of the atmosphere from the altitude of several hundred kilometers (along the vertical line) constitute about $(2\div 4) \cdot 10^{-2}$ rad, and the devices must have the angular solution, at least $(2\div 4) \cdot 10^{-3}$ rad in order to expose the character of high-altitude distribution of the intensity of the atmospheric radiation.

Difficulties connected with the registration of infrared radiation obtained from cosmic apparatus, limit the possibilities of similar investigations. For example, in experiments [1,2] the radiation was studied with the aid of radiometers in various sections of the spectrum in the ~ 0.1 rad angle and in essence only the data in the direction of nadir were used. In the experiment [3] the visual angle was still greater (about 0.3 rad) and the spectrum in the range 1.8-15 micrometers was studied. In the experiment [4] a compromise decision has been reached -- the visual angle constituted about $4 \cdot 10^{-2}$ rad during the registration of the spectrum in the broad range (from 7 to 38 micrometers). However, a very slow scanning along the spectrum during the sighting at nadir, has taken place here, which, in essence, limited the amount of information obtained from sections with uniform conditions existing in the atmosphere.

In our previous work [5] results of studies of the Earth's radiation were cited, which were obtained with the aid of scanning equipment, with sufficiently low visual angle ($2 \cdot 10^{-3}$ rad) which equipment permitted one to register, with adequate speed (~ 0.1 sec/spectrum) the spectral distribution in several sections in the 0.8-38 micrometers range (at best with solution ± 2 micrometers); all spectral sections were surveyed during the registration time in the range of permissible

angle without the displacement in space. However, this experiment was instrumental only in studying the high-altitude course and the atmospheric radiation field in the limited area and for the limited set of circumstances, inasmuch as the apparatus was ascending vertically on the directed geophysical rockets. By conducting experiments on the sputnik one can expand the climatic-and-geographic set of conditions in the atmosphere.

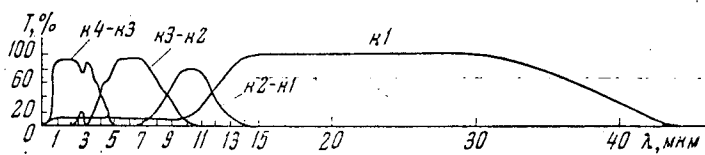


Fig. 1. The passage of spectral intervals of a scanning spectrometer.
k1:12.5-38 micrometers; k2-k1:8.5-12.5 micrometers; k3-k2:4.5-8.5 micrometers; k4-k3:0.8-4.5 micrometers.

2. Results of the experiment conducted on the "Kosmos-45" satellite, September 13, 1964 are cited in the current work. The experiment has been limited as to the time and it has not pursued meteorological aims.

The infrared spectrometer, installed aboard the satellite, was guided vertically, and its optical system carried out the scanning within the $\pm \pi/2$ angle from nadir, and registered radiation from the lower hemisphere. The characteristics and the principle of operation of spectrometer are similar to that described in [5]. In particular, the visual angle in the scanning plane located in a position perpendicular to the plane of the orbit, constituted $2 \cdot 10^{-3}$ rad, the scanning speed $2 \cdot 10^{-2}$ rad/sec.

Reproduced from
best available copy.

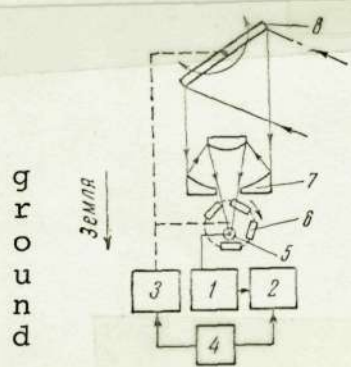


Fig. 2

Fig. 3

Fig. 2 - Block-diagram of a scanning pulse spectrometer

1 = amplifier, 2 = loop oscillograph, 3 = drive,
4 = program device, 5 = pointmeter, 6 = modulator
7 = lens, 8 = scanning mirror

Fig. 3 - General view of scanning spectrometer

1 = electronic-optical unit, 2 = oscillograph,
3 = program device.

Four spectral intervals 0.8-38 micrometers, 4.5-38 micrometers, 8.5-38 micrometers, 12.5-38 micrometers have been registered during approximately 0.10 sec time corresponding to the shifting of optical system per angle $2 \cdot 10^{-3}$ rad. As a result of aftertreatment three more intervals were isolated: 0.8-4.5 micrometers, 4.5-8.5 micrometers and 8.5-12.5 micrometers. Spectral distribution of Earth's radiation has been studied according to four intervals: 0.8-4.5 micrometers, 8.5-12.5 micrometers and 12.5-38 micrometers. The 4.5-38 micrometer interval characterized the integral thermal radiation of the Earth. Passage of the spectrometer in single spectral intervals is shown in figure 1. The use of the illuminating power method of monochromatization was instrumental in reaching the accuracy of measuring the stream in separate sections ± 2 micrometers $\sim 6\%$ wide, with the accuracy of registration of integral radiation 1% (which corresponds to the change of effective temperature of the radiating object 0° , 8K). The effective angle resolution (by considering optical and electrical characteristics) constituted $5 \cdot 10^{-3}$ rad during the registration time of one resolved 25 millisecond element.

Similar high speed required the passage zone of the recording installation of about 200 hertz. Absorbing plates of the modulator, with the aid of which the separation of individual sections of the spectrum has been accomplished, by intersecting the radiation beam, produce at the emergence from

the receiver -- the quick-response Colometer -- a signal of impulsive form. After being reinforced by electronic intensifier, the signal has been registered on the film of a small-scale loop oscillograph. After the termination of the experiment the film has been returned to Earth in a special container. The indispensable rate of the lasting of the film in the oscillograph, selected from among the quick-acting conditions of a spectrometer, constituted 25 mm/sec, which required the development of an oscillograph with a cassette that could hold up to 100 m of film. In order to encompass a possibly larger number of various areas during long-term flight a distinct registration was used. After two consecutive surveys at the angle $\pi/4$, the scanning spectrometer and expansion have been stopped and subsequently switched on after 10-15 minutes of the flight. Switching on and off, the equipment has been carried out by a specially scheduled device.

A block diagram of the equipment is shown in figure 2, and its general appearance -- in figure 3. The basic unit of this equipment is a collecting and intensifying device. A quick-response Colometer has a rectifying capability $D^*=1.5 \cdot 10^9$ (hertz.cm) $1/2$ /watt with time constant 5-7 microsecond, resistance 1,000 ohm, and the size of receiving platform $0.3 \times 9\text{mm}^2$. The amplifier on the economical core-type electron tubes (figure 4) has intensification about 10^6 with the filter zone

0.5-200 hertz. The amplifier is feeding two oscillograph circuits, which fact makes it possible to have two sensitivity scales of the device. An automatic sensitivity control over the optical system's inlet is provided in the equipment by means of periodic introduction of a signal from the calibrating tube. The value of the calibrating signal considerably exceeds that of the flow from the modulator, in order to disconnect the influence of its own thermal flow. Therefore, during the introduction of calibrating signal the sensitivity of the amplifier decreases automatically (to preserve one and the same scale) and a prescribed number of times by means of switching connection relay K_6 .

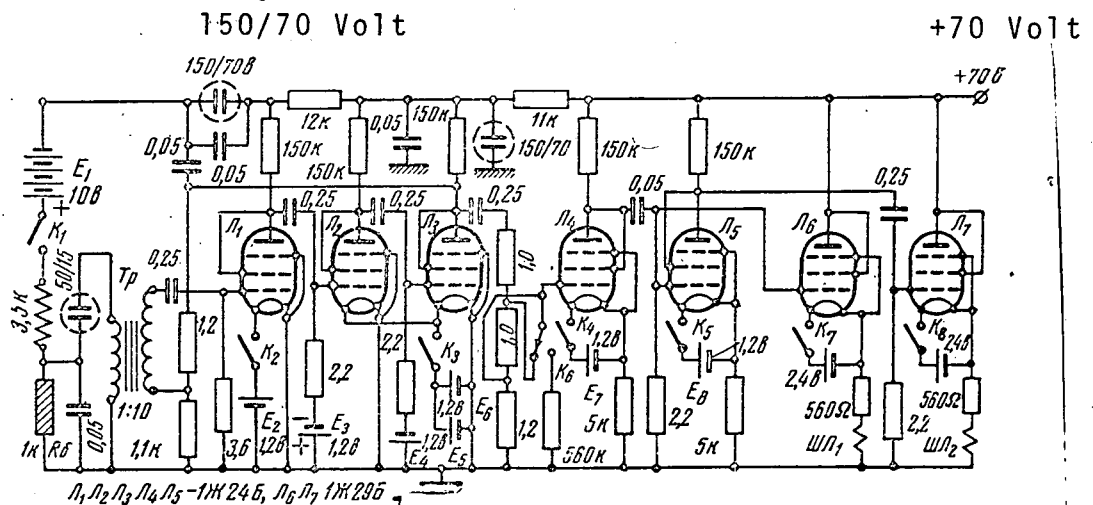


Fig. 4. Schematic drawing of a receiving-and-amplifying installation.

Incandescence circuits of electron tubes and Colometer power supply are switched on by the relay contacts. The total input of the receiving-and-amplifying installation is about 0.5 watt. The threshold sensitivity of an amplifier is 10^{-9}

v/hertz. The amplifier is thoroughly screened off by multi-layer Permalloy shields. It is significant that the sensitivity of a receiving-and-amplifying installation with electron tubes and metal Colometer remains constant with extensive temperature variations of the surrounding environment. The aggregate weight of the whole equipment amounts to about 10 kilograms (force).

3. The equipment has functioned over a period of one loop and, during that time, there have been obtained characteristics of the radiation field in the seven areas of the globe. The scanning routes and also wind force, cloudiness and ultimate temperatures (in the absolute scale) for the seven operation cycles of the device are shown in figure 5. The cycles are marked down by heavy lines. Here is also shown the terminator line for the mean time of the loop ($18^h 10^m$). Aside from these informations it is necessary to note that a developed spiral-like cloud system for the cycle No. 2 (Japan) existed in the area of observation according to television photographs of the "Tyros" satellite. As it can be seen in figure 5, a half of obtained information pertains to the night side of the globe, and one scanning cycle pertains to the terminator's zone. Three cycles were conducted in the Northern Hemisphere, three in the Southern and one in equatorial zone. Almost three cycles encompass continental areas, the remaining ones basically correspond to oceanic regions. Thus obtained

data characterize a broad collection of climatic and geographic conditions. It should be noted that scanning at the angle $\pi/4$ has been carried out twice during every cycle of operation, and areas extending for several thousand kilometers have been surveyed.

About 10,000 spectra of high quality have been obtained in all. The sample of record obtained during the flight is cited in figure 6,a. A series of impulses per several revolutions of the modulator is shown in figure 6,b. Curves of angular distribution for flows and effective temperatures with the aid of procedure described in [5] have been constructed according to these data. Likewise, there the current corresponds to the radiation of the square meter of the Earth in the hemisphere (in watt/m²) in the assumption of its isotropic distribution over the angles, and the effective temperature matches up the temperature of the absolute black substance, radiating the flow equal to the surveyed one. Generally speaking, the similar definition is correct for integral radiation ($\Delta\lambda = 0-\infty$), however, in view of the fact that sections of the spectrum examined in our case are comparatively extensive and distribution within the bounds is known to be not uniform, the introduction of effective temperature is expedient in restricted sections of the spectrum ($\Delta\lambda \equiv \lambda_2 - \lambda_1$) also conforming to radiation. The general character of the curves of angular distribution is similar to that previously

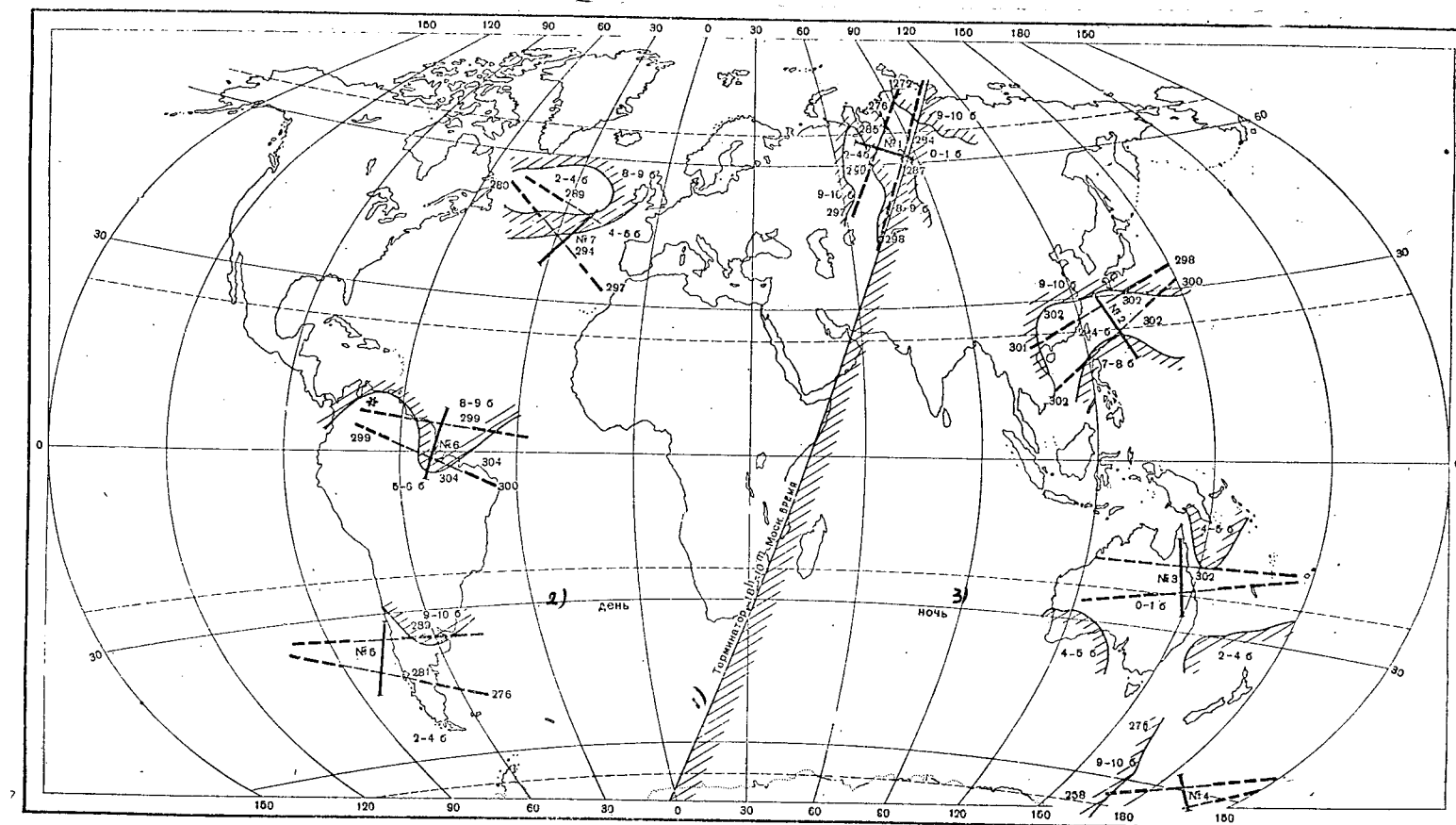


Fig. 5. Scanning routes during 13 Sept. 1964 experiment

1. Terminator 18h-10m Moscow time
2. day
3. night

Reproduced from
best available copy.

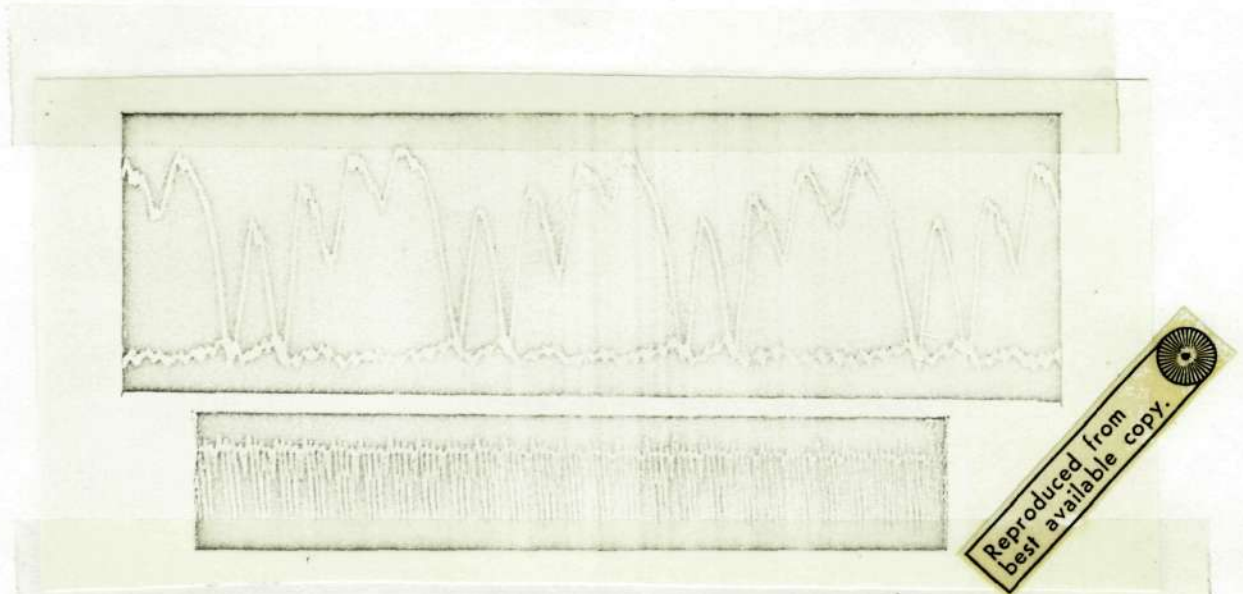


Fig. 6. The sample of the entry during the flight (a); a series of impulses during several revolutions of a modulator (b).

A section of the processed record of the angular distribution curve in various spectral intervals for the cycle No. 6 is presented in figure 7. Here, side by side with the significance of flows and effective temperatures values of albedo are given, computed for the channel 0.8-4.5 micrometers, with the mean Sun's altitude during the cycle (in all cases radiation and reflexion indices according to Lambert are accepted for the atmosphere). The section of the scanning course corresponding to the cited curves, is marked by an asterisk in figure 5. In figure 7 the angle scale has an arbitrary reading origin, whereupon the angle increase is corresponding to the proximity of the course of sighting towards the nadir.

4. Various components of the atmosphere bring their contributions to the radiation in definite sections of the spectrum. We shall study from this point of view separate channels of spectrometer's passage.

a) Channel 4 - channel 3 (0.8-4.5 micrometers).

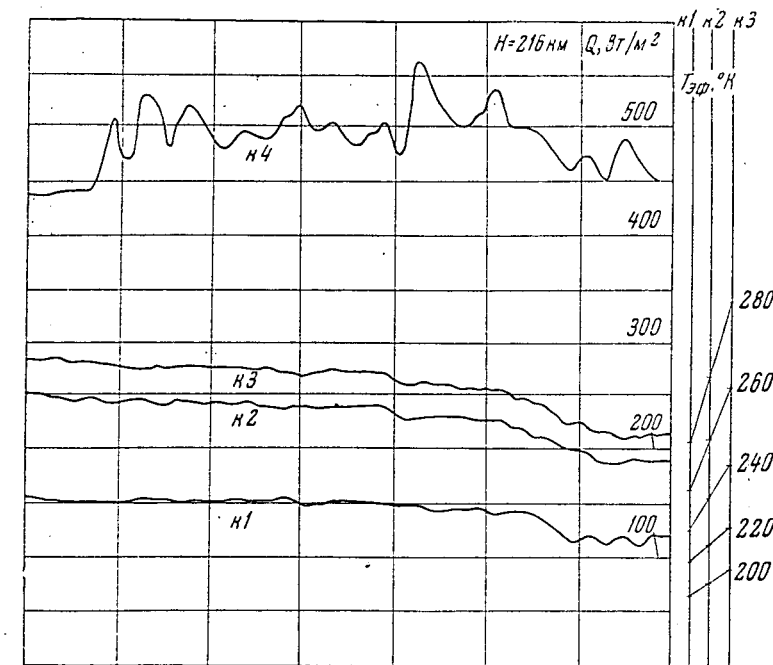
About one half of energy coming from the Sun is concentrated in this section of the spectrum. The contribution of thermal radiation of the Earth is very small here (fractions of percentage from the Earth's full flow). Hydroxyl radiation is possible in the higher layers of the atmosphere. In conformity with [6] the most intense belts of absorption ON are situated in the 2.9-3.0 micrometers zone (passages 1- 0.2 -1).

According to the data [7] the radiation of the nocturnal sky is observed in the 1.5-2.5 micrometers zone, which is identified with belts ON (passages 3-1, 4-2, 5-3, 9-7 etc.). The intensity of this radiation according to observations [8] (belts 4-2, 5-3, 3-1) comprises $3 \cdot 10^{-4}$ watt/cm² micrometers, and according to the data [7] for the same belts $2.5 \cdot 10^{-3}$ watt/cm² micrometers.

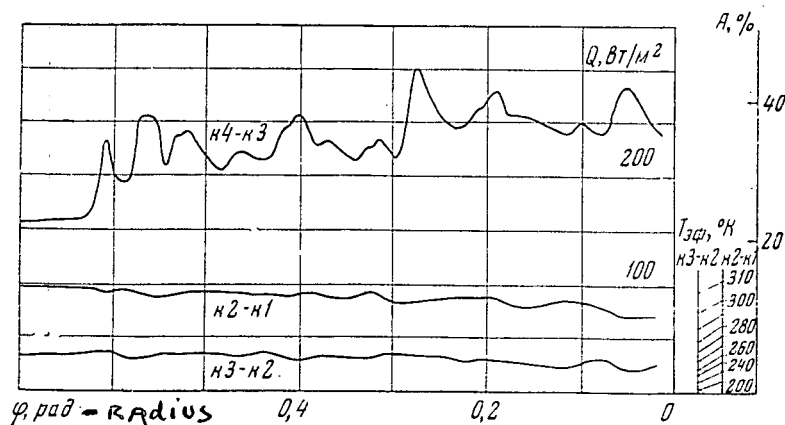
If one considers that the intensity of belts 1-0.2, 2-1 is twenty times higher (this follows from the computation [6]), so potential radiation flows ON in the 2.5-3 micrometers field ON reach during the night $5 \cdot 10^{-2}$ WATT/m² micrometers according to [7], or $6 \cdot 10^{-3}$ WATT/m² micrometers [8].

b) Channel 3 - channel 2 (4.5-8.5 micrometers).

About 10% of the radiation energy of the Earth is enclosed in this area of the spectrum for the effective temperature 250°K. The most intense absorption belts of vapors H_2O ($\lambda_0 = 6.3$ micrometers), NO ($\lambda_0 = 5.3$ micrometers), N_2O ($\lambda_0 = 4.7$ and 7.8 micrometers), CH_4 ($\lambda_0 = 7.8$ micrometers) and less intense belts OH ($\lambda_0 = 4.5$ micrometers) are concentrated here.



H=216 км Q, WATT/m²



Q WATT/m²

TEF

Fig. 7. Section of the angular distribution curve for the cycle of operation No. 6.

Under conditions existing near the ground (up to 10 km) an extremely extensive belt of water vapors gives the greatest contribution in this zone of the spectrum. However, its extension substantially decreases for greater altitudes [9] and, apparently, the radiation of other components begins to play part to an equal degree. The contribution to a general flow will be determined by temperatures and high-level distribution of all basic radiation components of the atmosphere. It is necessary to take into consideration the fact that the concentration of water vapors very rapidly decreases with the altitude, at least, till the level of tropopause is reached due to the drop in temperature and in condensation process.

c) Channel 2 - channel 1 (8.5-12.5 micrometers). This field of spectrum corresponds to the so-called - - - - (omission in text) of the atmosphere. The absorption here apparently is basically determined by water vapors (by wings of belts localized in other sections of the spectrum) and a belt O_3 ($\lambda_0 = 9.6$ micrometers). The contribution of belt O_3 , is, however, not great ($\Delta\lambda \sim 0.5$ micrometers), in any rate not higher than 10-15%. It should be noted that approximately in 75% of cases in this field of the spectrum, the radiation of the upper boundary line of clouds is registered. The radiation of the atmosphere near the ground (0-2 km) and in the underlying

surface is forthcoming, however, only in areas with a low water vapor content.

d) Channel 1 (12.5-38 micrometers). In this extensive field of the spectrum are concentrated absorption belts CO_2 ($\lambda_0 = 15$ micrometers) and the rotational spectrum of water vapors. The distribution of carbon dioxide along the altitude has been comparatively well learned, and the estimates of the effective radiation level (considering modification of absorption coefficient with altitude) show that the flow is generated by low-temperature layers ($T \sim 200-220^\circ\text{K}$). Measurements confirm this [4]. Besides, the width of the spectrum CO_2 is not great (2-3 micrometers). The effective temperature of the water vapors' radiation, as a rule, is higher (according to the data [1] up to 250°K), and the width of the water vapors spectrum is not less here than 12-15 micrometers. Thus, water vapors mainly (80-90%) furnish their contribution to the radiation of the spectrum section under consideration.

5. It is most convenient to analyze for various ranges of sighting angles results of the conducted experiment. The peculiarities of the Earth's radiation field are of particular interest: (a) in the field of angles not much differing from the nadir (up to 1 ± 1.5 rad), (b) in angles adjacent to horizontal direction. In the first case the results characterize the total study of the Earth and the atmosphere (including also

the clouds), in the second - the radiation of free atmosphere and, in particular, the ionosphere. The study of total radiation and its climatic and geographic variations in case under consideration represents an interest, as no full knowledge pertaining to radiative peculiarities of various climatic and geographic zones is available, especially of those obtained with high spatial resolving power (up to $5 \cdot 10^{-3}$ rad).

a) We shall at first examine absolute values of flows and effective temperatures, and also their variations for essentially different climatic and geographic zones in directions, close to the nadir. Moreover, it is expedient to average vibrations of flows in $0.2-0.3$ rad angles in order to increase the statistical accuracy. All together it has been possible to utilize the data for 27 zones of the globe, with distances among them from 1,000 to 4,000 km. Out of that number 13 zones are in the Northern Hemisphere, 14 in the Southern, 12 in the night side, 11 in the daytime side and 4 are in the terminator area. Twelve continental and 15 oceanic zones of the globe differ essentially as to the conditions of underlying surface. The sighting angles for all those zones constitute $0.6-0.8$ rad from the nadir.

In table 4 data are cited for the flows Q , for effective temperatures T_{ef} and spectral densities of radiation I , obtained as a result of averaging for all 27 zones of the

globe, and also separately for the Northern and Southern Hemispheres, for the night and day, for continents and oceans. These data have been obtained for the ranges 4.5-38 micrometers (integral flow), 4.5-8.5 micrometers, 8.5-12.5 micrometers and 12.5-38 micrometers. The value of integral flow on the average in each planet constitutes 245 WATT/m^2 , and the corresponding value of effective temperature is 255°K .

Little variability of these values during wide variations in observation conditions attracts attention. They practically remain constant during the day and at night in the Southern and Northern Hemispheres and are somewhat higher in continental areas in comparison with oceanic ones. The latitudinal course has been established very roughly due to the small number of points. Nevertheless, one can note that the mean value of integral flow in the field of latitudes adjacent to the equator ($\pm 15^\circ$) constitutes about 290 WATT/m^2 (265°K), in the middle latitudes $220\text{-}260 \text{ WATT/m}^2$, and finally, in high latitudes (70°) declines $200\text{-}210 \text{ WATT/m}^2$. In the zone of the spectrum 8.5-12.5 micrometers, that corresponds to the "transparency window" of the atmosphere, the value of the flow on the average in the planet constitutes 62 WATT/m^2 , and the effective temperature 276°K . Flow and temperature variations in this region of the spectrum are the greatest; the flows are higher in the daytime, in the continental areas and in the Southern Hemisphere.

Mean effective temperatures for the region of the spectrum 8.5-12.5 micrometers can be compared with the corresponding data from [1,2], averaged in 5 zones of the globe, where the effective temperature 274°K has been obtained. Approximately similar mean effective temperatures have been obtained for the section about 9.5 micrometers in the operation [4]. In the majority of cases effective temperatures in this section of the spectrum are lower than those of underlying surfaces. However, there are zones where these temperatures are close. Out of the total number of registered cases, approximately in 20% actual and effective temperatures differ by $2-5^{\circ}\text{K}$, in 50% by $15-20^{\circ}\text{K}$, in 20% by 30°K and in other cases more than by 30°K up to $60-70^{\circ}\text{K}$. So, for example, the proximity of actual and effective temperatures can be observed in the region of the Australian desert with a dry, clear atmosphere (cloudiness 0-1 points), and also (which is more unexpected) in the region of the equatorial part of South America, where, generally speaking, the surface moisture is greater and where mean conditions of cloudiness (5-6 points) have been observed. Thus, the transparency of the atmosphere in the 8.5-12.5 micrometers range in majority of cases constitutes only 50-70% and sometimes decreases still more. Of course, the question is about the effective transparency of the atmosphere on the average with regard for the presence of a definite degree of cloudiness. In figure 8 is cited the relation of the effective temperature

in the 8.5-12.5 micrometers range to the actual temperature of the underlying surface for all regions where surveys have been conducted that illustrated the carried out deductions. It is necessary to note that the temperatures of underlying surface may partially not satisfy the requirements of surveys made on the sputnik, due to the difference in time of synoptic data and measurements obtained.

1	2	3	4
Области спектра, мкм	Q, Вт/м ²	T _{эф} , °K	I, Вт/м ² мкм
Северное полушарие 5			
4,5--38	243	254,5	7,25
4,5--8,5	36	268	9
8,5--12,5	56	271	14
12,5--38	138	245,5	5,4
Южное полушарие 6			
4,5--38	247	255,5	7,38
4,5--8,5	53	284	13,3
8,5--12,5	66	281	16,5
12,5--38	135	244,5	5,3
День 7			
4,5--38	245	255	7,3
4,5--8,5	33	265	8,25
8,5--12,5	64	279	16
12,5--38	144	249	5,65
Ночь 8			
4,5--38	245	255	7,3
4,5--8,5	57	287	14,2
8,5--12,5	57	273	14,2
12,5--38	139	241	5,45
Материки 9			
4,5--38	267	261	8
4,5--8,5	48	279	12
8,5--12,5	78	283	18,1
12,5--38	146	254	5,7
Океаны 10			
4,5--38	222	250	6
4,5--8,5	44,7	276	11,2
8,5--12,5	55,3	268	13,8
12,5--38	123	238	4,8
Среднее 11			
4,5--38	245	255	7,3
4,5--8,5	45	277	11
8,5--12,5	62	276	15,5
12,5--38	137	245	5,35

Table I

1. Zones of the spectrum, micrometers
2. Q, WATT/m²
3. T_{ef}, °K
4. I WATT/m² micrometers
5. Northern Hemisphere
6. Southern Hemisphere
7. Day
8. Night
9. Continents
10. Oceans
11. Mean

In the zone of the spectrum 12.5-38 micrometers the effective temperature on the planet, on the average, constitutes 245°K , it is practically invariable for the Northern and Southern Hemispheres, and is a little higher in the daytime than at night, and in the continental zones in comparison with oceanic ones. This temperature is close to the mean effective temperature of water vapors (242°K), obtained in [1,2] for the zone 6.3 micrometers ($\Delta\lambda=0.5$ micrometers). However, it is necessary to consider, that in the 12.5-38 micrometers zone, besides water vapors, the carbon dioxide radiates ($\Delta\lambda=2-3$ micrometers) with a lower temperature. The elimination of carbon dioxide radiation flow increases the effective temperature of water vapors up to $250-260^{\circ}\text{K}$.

As far as results are concerned the most interesting is the zone of spectrum 4.5-8.5 micrometers. The mean effective temperature on the planet in this case constitutes 277°K , which is essentially higher than the expected temperature. Should the basic contribution in the radiation of this zone be provided by water vapors in the upper troposphere and in stratosphere. Radiation of the water vapors of the lower troposphere cannot play a noticeable part, as the absorption coefficient of water vapors in the zone 6 micrometers is such that in the atmospheric layers at the 7-10 km altitude the transparency is very small. The effective temperature in this zone of the spectrum in the Southern Hemisphere proved to be

considerably higher than in the Northern (284 and 268°K) and, which is very interesting, is higher at night than in the daytime (287 and 265°K).

T_{ef} , °K

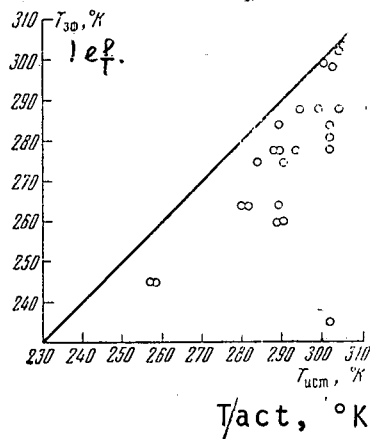


Fig. 8. Relation of effective temperature in the 8.5-12.5 micrometers range to active temperature of the underlying surface.

The correlation of data (in particular of effective temperatures) in various zones of the spectrum is of essential importance concerning the interpretation of obtained results. In the theoretical plan for radiation in the outer space of the Earth it is assumed that the maximum radiation is concentrated in the zone 8-12 micrometers. It is connected with the idea that the atmosphere here is relatively transparent, the underlying surface has temperatures, corresponding to the maximum radiation also in this section of the spectrum, and their value is considerably higher than the temperatures of upper troposphere [10]. As the conducted surveys have shown, often an experimentally observed picture satisfies the requirements of this plan.

However, the data obtained by us, including those in work [5], enlarge it substantially. It has been found out that, in 20-30% of cases, considerable deviations are observed consisting in the presence of temperature inversion, established in flows in zones 4.5-8.5 micrometers and 8.5-12.5 micrometers: effective temperatures, determined according to radiation in the first zone, surpass effective temperatures discovered in the "transparency window" in connection with radiation. Similar inversion can also be seen in the data [1,2]. As a rule, the inversion exists in the zones of high-power cloud systems, where the radiation intensity in the "transparency window" is not great. The significant difference of our data is such that very high effective temperatures in the section of the spectrum 4.5-8.5 micrometers are observed and the inversion value is considerable and it sometimes reaches 40-45°K. In the table 2 is cited a correlation of effective temperatures in various sections of the spectrum for characteristic cases of presence and absence of inversion. It should be noted that the presence of inversion corresponds to a high-power spiral-like cloudiness in the zone of the cycle No. 2 and to a considerable cloudiness in the Antarctic regions (cycle No. 4), whereupon both of these cases are attributed to the night side of the globe.

Table 2

1	2	3	4	5	6	7
Область спектра, мкм	$Q, \text{ вт/м}^2$	$T_{\text{эф}}, ^\circ\text{K}$	$I, \text{ вт/м}^2 \text{ мкм}$	$Q, \text{ вт/м}^2$	$T_{\text{эф}}, ^\circ\text{K}$	$I, \text{ вт/м}^2 \text{ мкм}$
Инверсия 8						
Цикл № 2 9				Цикл № 4 10		
4,5—8,5	50	282	12,5	57	286	14,2
8,5—12,5	25	235	6,25	34	245	8,5
12,5—38	80	210	3,2	100	225	3,9
4,5—38	175	230	5,2	180	235	5,4
Отсутствие инверсии 11						
Цикл № 6 12				Цикл № 7 13		
4,5—8,5	45	280	11,3	15	240	3,8
8,5—12,5	90	303	22,5	62	278	15,5
12,5—38	160	260	6,3	130	242	5,1
4,5—38	290	268	5,7	220	250	6,5

1. Zone of the spectrum micrometers
2. $Q, \text{ WATT/m}^2$
3. $T_{\text{ef}}, ^\circ\text{K}$
4. $I, \text{ WATT/m}^2 \text{ micrometers}$
5. $Q, \text{ WATT/m}^2$
6. $T_{\text{ef}}, ^\circ\text{K}$
7. $I, \text{ WATT/m}^2 \text{ micrometers}$
8. Inversion
9. Cycle No. 2
10. Cycle No. 4
11. Absence of inversion
12. Cycle No. 6
13. Cycle No. 7

Correlation of effective temperatures for various sections of the spectrum which are characterized by the radiation of specific atmosphere components, may impart certain information about the localization of pertinent radiating layer. In figure 9 the relation of effective temperatures is shown, determined in connection with the integral radiation, from effective temperatures, discovered in the "window of transparency". Despite the limited number of points, a definite relation is made apparent. In figure 10 a similar relation is listed for sections of the spectrum 8.5-12.5 and 12.5-38 micrometers. As can be seen here, a correlation of effective temperatures also exists here, though these are already independent intervals of wavelengths. In figure 11 and 12 are shown relations for sections 4.5-8.5 and 8.5-12.5 micrometers, and also 4.5-8.5 and 12.5-38 micrometers. Here the correlation is practically non-existent. Thus, one can infer that there also exists a contribution of identical components of the atmosphere in flows generated in spectral zones 8.5-12.5 and 12.5-38 micrometers.

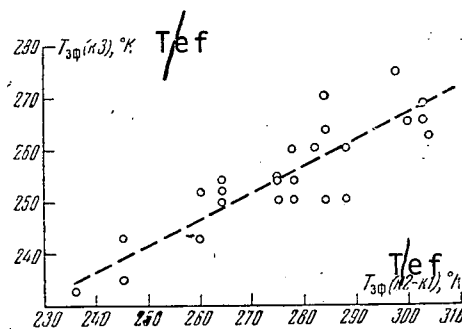


Fig. 9. Relation of effective temperature, determined according to radiation in the section of the spectrum 4.5-38 micrometers to the effective channel temperature 8.5-12.5 micrometers.

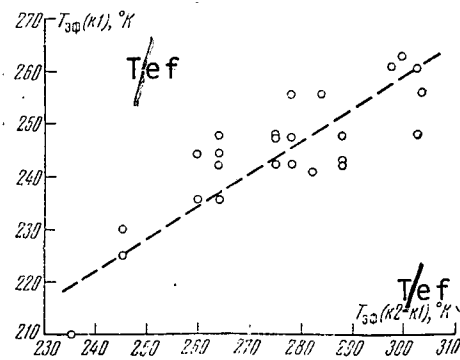
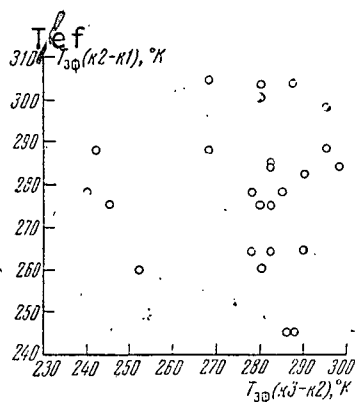
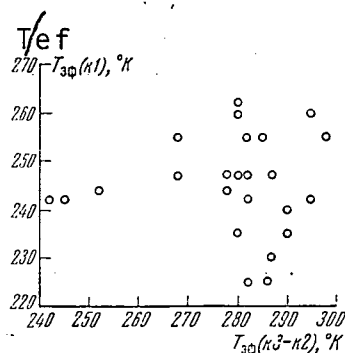


Fig. 10. Relation of the effective temperature of the channel 12.5-38 micrometers to the effective temperature of the channel 4.5-8.5 micrometers.



$T_{ef} (K3-K2) ^\circ K$

Fig. 11. Relation of the effective temperature of the channel 8.5-12.5 micrometers to the effective temperature of the channel 4.5-8.5 micrometers.



$T_{ef} (K3-K2) ^\circ K$

Fig. 12. Relation of the effective temperature of the channel 12.5-38 micrometers to the effective temperature of the channel 4.5-8.5 micrometers.

However, the flow in the zone 4.5-8.5 micrometers is generated by the components of atmosphere that practically do not give any contribution in other sections of the spectrum. It is known that water vapors and carbon dioxide are common components in these zones of the spectrum. However, the contribution of the zone CO_2 in the section 4.5-8.5 micrometers is very small (only the wing of the zone is possible). The contribution of water vapors is apparently small, as their temperature is not great. Therefore, the radiation basically should be determined by other substance. It is possible that H_2O dissociation products, for example OH, possibly NO or N_2O . The interval of elevations, where radiation is generated in conformity with effective temperatures, constitutes 50÷60 km.

Side by side with peculiarities of spectral variations of the Earth's radiation field, statistical data on variation of flows and temperatures for all climatic and geographic regions are of interest. Such data are collected in table 3, where maximum, minimum and mean values of Q flows and effective temperatures T_{ef} , also root-mean-square deflections of these values from the mean. Relations of amplitude to dispersion, that characterize the type of distribution are presented in the table. This relation is close to 5 for normal distribution. As it is seen, effective temperatures determined after the flow into the "transparency window" undergo maximum fluctuations, and integral temperatures are subjected to minimum fluctuations. Everywhere the type of distribution somewhat differs from the normal one.

Information obtained in the given experiment in reference to albedo permit one to investigate the problem about the correlation of meteorological situation to the level of thermal radiation and also to determine the thermal balance in investigated zones. The value of the albedo of the Earth essentially depends on the cloud cover, whereupon this is all the more true in the investigated areas of the globe (cycles No. 5, 6, and 7), as the areas with underlying surface, covered with snow or ice are not encompassed by observations. The value of the data is advancing in connection with the fact that

the reflected and thermal radiations have been registered by the same device with one optical system and receiver, possessing very high spatial solution capability (10^{-4} rad²). Values of the integral flow of thermal radiation Q rad and albedo A for three daytime operation cycles and for the arbitrary sighting directions within 0.3-0.8 rad angles from the nadir are presented in table 4 and averaged according to the 0.2-0.3 rad angle. In the same table flows of solar radiation, absorbed by the Earth Q absorb are shown, also data on cloudiness and the character of underlying surface in areas where surveys have been conducted. It is necessary to note the tentative character of these data, inasmuch as they can differ by several hours in time with those surveyed.

Table 3

Currents, temperatures	Spectrum region, mkm			
	4,5 — 38	4,5 — 8,5	8,5 — 12,5	12,5 — 38
$Q_{\text{maximum}} W/m^2$	320	75	95	165
$Q_{\text{minimum}} W/m^2$	175	15	25	80
$Q_{\text{average}} W/m^2$	245	45	62	137
$Q_{\text{through}} = \sqrt{(Q - Q_{\text{avg}})^2}, W/m^2$	35	14,8	17,5	19,5
$T_{\text{ef.max.}} ^\circ K$	275	298	304	262
$T_{\text{ef.min.}} ^\circ K$	233	240	235	210
$T_{\text{ef.av.}} ^\circ K$	255	277	276	245
$T_{\text{ef.thr.}} = \sqrt{(T_{\text{ef.}} - T_{\text{ef.av.}})^2}, ^\circ K$	8,8	14,8	17,7	11,7
$Q_{\text{max}} - Q_{\text{min}}$	4,15	4,05	4,0	4,35
Q_{through}				
$T_{\text{ef.max.}} - T_{\text{ef.min.}}$	4,8	3,9	3,9	4,45
$T_{\text{ef.through}}$				

Reproduced from
best available copy.



Table 4.

$Q_{\text{zad}}, \frac{\text{W}}{\text{m}^2}$	$A, \%$	$Q_{\text{abs}}, \frac{\text{W}}{\text{m}^2}$	Charac. of under- line surface	Cloudiness points
Cycle № 5, $z = 53^\circ$, 10 ^h local time				
220	62	320	ocean	2-4
225	70	250	»	»
200	90	84	»	»
200	60	340	»	»
225	50	420	land, steppe/	9-10
150	30	590	ocean	2-4
Cycle № 6, $z = 17^\circ$, 12 ^h local time				
300	32	920	land, forest	5-6
270	50	675	»	»
280	45	745	»	»
250	45	745	»	»
280	25	1000	»	»
220	40	810	»	»
320	10	1210	ocean	»
Cycle № 7, $z = 41^\circ$, 14 ^h local time				
220	50	525	ocean	4-5
220	15	900	»	8-9
170	30	740	»	2-4
210	18	860	»	»
180	25	790	»	»

From data cited in table 4 one can see, that the mean albedo constitutes 39%, the mean absorbed flow from the Sun about 600 WATT/m² and the outgoing thermal flow about 230 WATT/m². With the exception of one case everywhere the gain in heat is greater than its expenditure. The case of the excess of expenditure corresponds to a very high value of albedo, and besides considerable large-scale (~ 0.2 rad) fluctuations of the albedo (10-20%) are observed in the zone where this occurs; at the same time small-scale fluctuations (< 0.1 rad) are negligible. A very mottled picture is presented while observations are made on relation of the Earth's thermal radiation's

level and the albedo. In majority of cases the motion of curves of the angular distribution in the field of 4.5-38 micrometers and even in the field 8.5-12.5 micrometers is considerably smoother than in the field 0.8-4.5 micrometers. The section of angular distribution curves presented in figure 7 serves as a typical illustration of this. Small-scale heterogeneities (of the order of 0.02 rad, i.e. about 10 km on the Earth) are practically absent in thermal radiation, while similar heterogeneities, as a rule, are present in the albedo and even reach 10% and more, as far as magnitude is concerned (at any rate their amplitudes are comparable to those of large-scale fluctuations). It is known that the spatial spectrum of atmosphere heterogeneities (clouds) has a lift in a low-frequency field. To a larger degree, this pertains to thermal heterogeneities in the atmosphere. All observed cases where correlation of thermal radiation and albedo has been studied can be divided into three groups: 1) increase or decrease of albedo corresponds to the decrease or increase of thermal flow, 2) increase or decrease of albedo corresponds to the increase or decrease of thermal flow and 3) correlation between the thermal flow level and albedo is absent. These three groups indicate various connections between the density, altitude and the amount of cloud formations in the atmosphere. Significant variations in the altitude of upper cloud boundary of

sufficiently great density correspond to the first group. Such variations of clouds in the altitude, when the character of cloudiness undergoes changes at the same time with the altitude, correspond to the second group. For example, there are high cirrus clouds with small albedo and low temperature, but well absorbing in the infrared field of the spectrum and, at the same time, there are low cumulus clouds with high albedo and temperature of upper boundary line. Cases of temperature inversion are also possible when the temperature nearby the upper boundary of dense clouds is higher than that of the underlying surface. Finally cloudiness variations with a very low upper boundary (several hundred meters, up to a kilometer) correspond to the third group.

The data according to groups are dispersed statistically in a following manner. The correlation is absent (55%) in the majority of cases, in some cases there is a dependence of the second group (30%), and, finally, a dependence of the first group (15%) in few cases. It is necessary to indicate that there is more often a connection between the flow and the albedo, characteristic of the first group for large-scale cloudiness and, at the same time, an independence for small-scale cloudiness. The number of cases, pertaining to the first group increases up to 30-40% for the thermal flow in the field of spectrum 8.5-12.5 micrometers. The correlation of the character of meteorological situation and of the thermal flow level for

the night side of the globe is possible to carry out only by attracting synoptic data. In this case it makes sense to conduct analysis only for large-scale cloud systems.

It is of interest here to separate two areas which are characterized by almost similar surface temperatures ($\sim 300^{\circ}\text{K}$), but essentially differ in a meteorological situation. This is the area of the cycle No. 2 (Japan), where a developed spiral-like cloud system has been observed, and the area of the cycle No. 3 (Australia), where clear weather predominated. The intensity of thermal radiation in cycle No. 2 rad over the large territory undergoes significant fluctuations. For example, the flow in the range 4.5-38 micrometers on the interval 0.2 rad fluctuates 1.5 times and in the range 8.5-12.5 micrometers 4 times. On the contrary, the radiation intensity during cycle No. 3 undergoes very little changes, even in the 8.5-12.5 micrometers range. The integral flow in the direction of 0.8 rad angle from nadir for the cycle No. 2 is on the average 240 WATT/m^2 , the effective temperature 250°K for the cycle No. 3 is correspondingly 290 WATT/m^2 and 268°K . Effective temperatures in the range 8.5-12.5 micrometers on the average constitute 270 and 293°K correspondingly.

b) While investigating the sighting angles range in the direction close to horizontal, first of all this fact attracts attention, that radiation, generated in enormous thicknesses (up to 1,000 km) enters into the visual field of

of the device. This circumstance signifies that even with negligible concentrations of the substance at great altitudes in the atmosphere, the intensity of radiation, determined by temperature and the number of radiating particles, may reach appreciable values. The study pertaining to curves of angular distribution, obtained with the equipment, that possesses high spatial solution, is a very sensitive method for analyzing high-altitude distribution of radiating atmospheric components in these directions. In our case, the device had angular solution, corresponding to the height of the atmosphere column at the distance of 1,500-2,000 km (from the device to the point of the Earth's contact), 5-7 km, which makes it possible to study comparatively well the structure of the atmosphere according to the altitude. In contrast to the sighting on the nadir, into field of vision of the device enters the radiation generated by various layers of the atmosphere situated above the level corresponding to the minimum distance of the surface of the Earth with the definite instantaneous direction of sighting. In addition to this, certainly, layers of the atmosphere in various all the time increasing altitudes will be situated along the optical course. Due to the sphericity of Earth the length of the course in the layer of atmosphere 5-7 km thick at the definite altitude comprises 400-500 km. The remaining course lies over more rarefied layers of atmosphere, nevertheless this circumstance may somewhat lubricate the

localization according to the altitude of the specific radiating layer.

The general character of angular distribution curves of Earth's radiation is such, that, within sighting angles from the nadir to the contact with the hard surface of the Earth, a slow decrease of radiation intensity (darkening towards the edge of the planet) is observed, and later sudden drop in intensity during the transition to the free atmosphere. Computations show that the form of the curve in this zone of angles for the surface atmosphere (30-40 km) depends essentially on the spectrum range [11]. As our previous investigations have shown, this is actually so [5], but the real atmosphere with great optical thicknesses requires that the estimate of radiation contribution in considerably greater altitudes should be made.

The analysis of data in the angular latitude of free radiating atmosphere (or, which is the same, of the effective altitude of radiating atmosphere) has shown the essential relation of this altitude to the surface climatic and geographic conditions. Already in experiments described in [5] the dependence on the surface concentration of water vapor has been made apparent. However, the accumulation of conditions there was limited, which fact did not permit one to talk about the universal function of such type. In the experiment under consideration, the surface conditions varied much more widely.

In particular, approximately one half of zones where surveys have been conducted corresponded to continental areas, one half to oceanic ones. The estimation of the altitude of the radiating atmosphere according to angular distribution curves in the spectrum sections, corresponding to the water vapor absorption belts, has shown that, in all cases where an aqueous surface exists in the sighting direction (over the territories comprising many hundreds or thousands of kilometers), the value of this altitude is greater than in those cases where continental areas exist in the sighting directions on Earth. This is especially manifested in the 12.5-38 micrometer range.

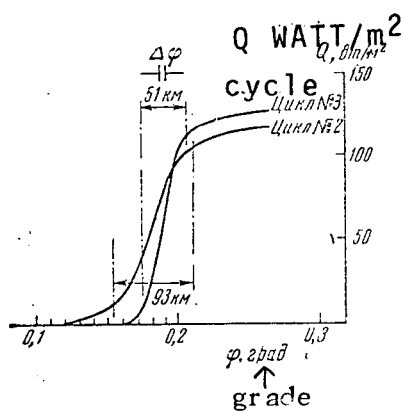


Fig. 13.

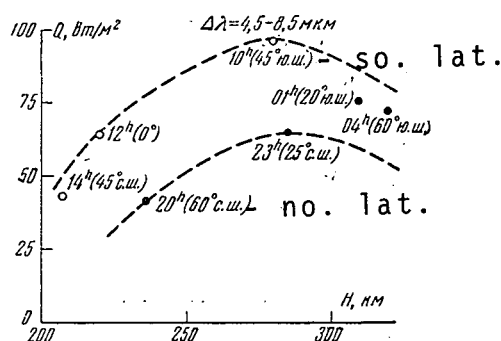


Fig. 14.

Figure 13. Angular distribution curves for the free atmosphere in the zone of the spectrum 12.5-38 micrometers with the continental (cycle No. 3) and oceanic (cycle No. 2) underlying surface.

Figure 14. High-altitude dependence of the ionosphere radiation in the zone of the spectrum 4.5-8.5 micrometers.

Sections of the angular distribution curves in the zone corresponding to the sighting of free atmosphere in the 12.5-38 micrometers range are presented in figure 13. A typical case, as an illustration, has been shown when one of the curves pertains to the area south of Japan (cycle 2), while the other one to the area of the Australian desert (cycle 3). As can be seen, the altitude of radiating atmosphere in the first case reaches 93 km and in the second 51 km (angular latitude is reckoned according to the levels comprising 10 and 90% from the maximum intensity). Thus the results of conducted investigations fully confirm previously expressed assumption [5] about the presence of water vapor in altitudes of the order of 100 km and about the relation of its concentration from the surface moisture over the great territories. It is necessary to note, that a similar correlation is never observed in the sections of the spectrum where the influence of water vapors' radiation is low (for example, in the "transparency window"), and the altitude of radiating atmosphere is considerably lower.

The use of the developed investigation method was instrumental in determining the presence of the infrared ionosphere radiation in elevations of 280, 420 and 500 km [12] localized in definite layers, of the order of 10 km thick. Investigation of this phenomenon in the zone of altitudes adjacent to 280 km was carried on in the present experiment. It is necessary to note, however, that, in the case under

consideration these investigations have been combined with a number of difficulties, connected, first of all, with a limited time of the service of equipment, and, secondly, with the presence of a twenty-four hour and latitudinal change occurring in the position of the sputnik with the change of the altitude. Therefore, obtained results can be studied as the preliminary ones. As in the work [5], it has been established, that basically the ionosphere infrared radiation is concentrated in the zone of the spectrum 4.5-8.5 micrometers. The relation of the intensity of the ionosphere radiation to the altitude of this section of the spectrum is presented in figure 14. Even those few points, which correspond to the seven cycles of the work of device, reveal maximum radiation at the 250-300 km altitude, when the radiation from the horizontal direction has been sighted. The intensity of daytime radiation of the ionosphere (bright nights) is considerably higher. However, even the radiation flows at night (dark nights) are considerable as to their absolute value. This circumstance that the high-altitude course essentially does not change during the considerable modification in latitude, apparently indicates that the ionosphere radiation has a weak latitudinal function. Values of the intensity of ionosphere radiation in various altitudes for 0.8-4.5 micrometers range are cited in figure 15. The essential difference here between the daytime and night flows does not permit one to construct altitudinal relation with the limited number of points. The

nature of discovered radiation is as yet not clear. Possibly, it is different for various spectrum sections. In this connection it is interesting to compare flows observed in the section of the spectrum 0.8-4.5 micrometers at night with the data of the surveys of the night sky radiations from the Earth [7,8] and with computations for belts OH[6]. In our case the night flows constitute 5-10 WATT/m². It is necessary to consider that the length of the optical course is 50-100 times greater than under conditions of surveys made from the Earth, where the radiation is observed not along but across the radiating layer. If the conversion is made pertaining to the conditions of surveys conducted from the Earth, we can assume that the radiation intensity for the rarefied gas is proportional to the number of particles and therefore to the length of the course, then the flow surveyed by us during observations conducted from the Earth will correspond to the flow 0.05-0.1 WATT/m². This not too drastically differs from the possible flows of night sky in the assumption of the radiation belts OH in the 2-3 micrometers zone, and it may testify to the fact that the radicals OH are responsible for the radiation of the ionosphere which has been observed by us in the zone of the spectrum 0.8-4.5 micrometers.

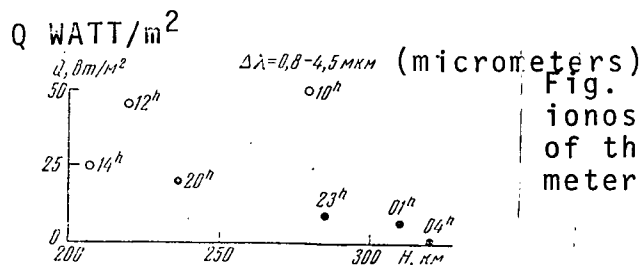


Fig. 15. The intensity of the ionosphere radiation in the zone of the spectrum 0.8-4.5 micrometers in various altitudes.

In the conclusion, it is necessary to note that the observed level of the integral infrared ionosphere radiation (0.8-38 micrometers) comprising about 150 WATT/m² corresponds to the comparatively calm condition of the Sun. Index of the magnetic field of the Earth K_p on 13 September was close to 1, and several days before the experiment only one or two weak explosions were registered near the central meridian of the disk of the Sun.

The date of the receipt

January 8, 1966

LITERATURE

1. W. R. Bandeen, R. A. Hanel, J. Licht, R. A. Stampfl, W. G. Stroud. J. Geophys. Res., 66, No. 10, 3169, 1961.
2. W. Nordberg, W. R. Bandeen, B. J. Conrath, V. Kunde, J. Persano. J. Atmosph. Sci., 19, No. 1, 20, 1962.
3. L. C. Block, A. S. Zachor. Appl. Opt., 3, 209, 1964.
4. A. N. Lebedinsky, D. I. Glovatskiy, V. I. Tulupov, B. V. Khlopov, A. A. Fomicheve, G. I. Shuster. Symposium Research of cosmic space. Publishing House "Nauka", 1965, p. 65.
5. P. A. Bazhulin, A. V. Kartashev, M. N. Markov. Symposium "Research of cosmic space". Publishing House "Nauka", 1965, p. 94.
6. I. S. Shklovskiy. News of the Crimean Astrophysical Observatory 7, 34, 1951.
7. I. F. Noxon, A. W. Harrison, A. V. Jones. J. Atmosph. Terr. Phys., 16, 246, 1959

8. V. I. Moroz. Reports of the U.S.S.R. Academy of Sciences, 126, No. 5, 983, 1959.
9. F. Stauffer, J. Strong. Appl. Opt., 1 No. 2, 129, 1962.
10. K. Ya Kondrat'yev, K. Ye. Yakushevskaya. Symposium "Problems of the physics of the atmosphere" issue 2, 1963, p. 48.
11. K. Ya. Kondrat'yev. Meteorological spectra. Gidro-meteoizdat. 1963.
12. M. N. Markov, Ya. I. Merson, M.R. Shamilev. Symposium "Research of cosmic space". Publishing House "Nauka", 1965, p. 112.

